Article

Protein nitration is a physiological regulator of cardiac lactate dehydrogenase active site loop mobility and activity

Cristian Nogales[1,*], Jeroen Frijhoff[1], Detlef Thoenges, Richard B. Sessions, Albert Sickmann, Tatiana Nedvetskaya, Cesar Ibarra-Alvarado, Vera Schmitz, Peter Rösen, Axel Goedecke, Aleksandar Jovanović, David H. Perlman, Anna Klinke, Stephan Baldus, Ana I. Casas, Péter Bai, Csaba Szabo, Martin Feelisch & Harald H.H.W. Schmidt[*].

[1]Both first authors contributed equally to this work.

[*]To whom correspondence may be addressed. Email: h.schmidt@maastrichtuniversity.nl or c.nogales@maastrichtuniversity.nl

Abstract (143 words)

Protein tyrosine nitration is considered one of the most relevant disease biomarkers of oxidative stress. The mechanism of nitration, target protein and functional consequences remain often unclear. We focus on a prominent protein band surprisingly nitrotyrosine immunopositive under basal conditions in mouse, rat and pig heart and more so in diabetes and myocardial stress. Upon purification, we identify it as lactate dehydrogenase (LDH) and its basal nitration depending on NO synthase (NOS) and myeloperoxidase (MPO), respectively. Surprisingly, we locate LDH nitration by MALDI-TOF mass spectrometry not to a tyrosine but the C-terminal tryptophan, Trp-324. Molecular dynamics simulations suggested that Trp-324 nitration restricts the interaction of the active site loop with the C-terminal α-helix essential for activity, which was corroborated by an apparent lower V_{max}. In summary, here we first extend protein nitration from pathology to physiology as an additional mechanism of post-translational regulation.

Increased levels of reactive oxygen species (ROS), i.e. oxidative stress, is considered a common mechanism of several cardiovascular and other disease states [1]. In concert with different nitrogen species [2–4], ROS can lead to protein nitration, e.g. tyrosine residues (NO_2Tyr). Tyrosine nitration is the most frequently used and considered the most robust disease marker of oxidative stress [5–7]. Its detection relies mainly on NO_2Tyr specific antibodies [8–10]. With respect to the nitrogen source, anti-NO_2Tyr immunopositive signals are generally interpreted as a hallmark of nitric oxide (NO) being scavenged by superoxide and intermediate peroxynitrite [9,11,12], although other mechanisms exist [13]. Regarding the functional consequences of protein nitration few *in vitro* data exist suggesting mainly loss of protein function correlating with disease severity [14–17]. *In vivo* data are lacking. Moreover, little is known about the protein factors that govern other nitration sites, e.g. tryptophan, and about the effects of the modification in protein structure and function [18]. Here, we address three major knowledge gaps in our understanding of protein nitration: specificity, origin, and disease relevance.

Results

Development of an anti-nitrotyrosine antibody panel as biomarkers of disease-relevant oxidative stress.

We started out by examining a panel of anti-NO_2Tyr antibodies (Fig. 1), including those directed against carrier-linked NO_2Tyr or against H_2O_2/NO_2^- treated proteins (see Supplementary Table 1). We tested these in rodent (rat) and, for later purification, also in porcine tissues. Surprisingly we obtained signals already under physiological conditions. The immunoreaction, however, varied greatly in protein band size and intensity. Two polyclonal (pAb), pAb1 and pAb2, and one monoclonal antibody (mAb), mAb1, displayed the most robust signals (Supplementary Fig. 1). The specificity of anti-NO_2Tyr antibodies [19–23] is rarely validated, e.g. by antibody pre-absorption with free NO_2Tyr [11]. In our case, pAb1 signals were partially blocked by pre-absorption with 3 mM NO_2Tyr. mAb1 showed very little non-specific background whilst pAb2 exhibited moderate sensitivity with high anti-NO_2Tyr specificity.

A prominent nitrotyrosine immunoreactive protein band was detected in mouse, rat and pig heart under physiological conditions.

To conduct a tissue/species screen, we selected three antibodies, pAb1, pAb2, and mAb1, from our original panel. Three proteins were consistently detected under basal conditions and with apparent molecular weights of 70, 45 and 38 kDa, of which the latter gave the by far the strongest signal in heart (Fig. 2a). Pre-incubation with free NO_2Tyr or NO_2BSA (3 mM) or nitro-group reduction [22], at least partially, blocked the pAb1 dependent signal. Therefore, subsequent efforts were directed at identifying the nature of the NO_2Tyr positive 38 kDa protein and its site of nitration.

Upon purification, the 38 kDa nitrated protein was identified as LDH with lower V_{max}.

Using porcine heart, we isolated the NO_2Tyr immunoreactive 38 kDa protein by ion exchange (Q Sepharose, QS) and affinity (Blue Sepharose, BS) chromatography (Fig. 2b). The partially purified 38 kDa protein was stained by colloidal Coomassie Blue and subjected to peptide mass fingerprinting using MALDI-TOF MS. Based on the NCBIprot database most ions present in the spectrum of tryptic peptides matched LDH as the primary protein component of the sample (Fig. 2c).

Next, we tested the effect of nitration on the enzyme activity by nitrating cardiac LDH *in vitro* with increasing amounts of H_2O_2/NO_2^-. Indeed, higher nitration levels of LDH (NO_2-LDH) (Fig. 2e) correlated with decreased V_{max} (Fig. 2f) and unchanged K_M. Our data suggest therefore that protein nitration is not only a physiological event for cardiac LDH, but also modulates enzyme activity by lowering V_{max}.

Nitrated LDH is increased in diabetes and myocardial stress.

To investigate whether NO_2-LDH is further increased in response to metabolic stress, we investigated heart extracts from rat models of streptozotocin-induced short-term (ST) and long-term (LT) diabetes mellitus [24] as well as a doxorubicin (DoxoR) induced mouse model of cardiac stress [25] (Fig. 3a). Diabetic rats were sacrificed 3 (ST) and 16 (LT) weeks after inducing diabetes at week 10. Using the pAb1, NO_2-LDH signals were significantly increased in all three models when compared against healthy controls (Fig. 3b-c). Immunosignals of pAb1 pre-absorbed with NO_2Tyr or anti-LDH wildtype antibody did not show any significant change. In both diabetes mellitus models and doxorubicin-treatment animals, levels of cardiac LDH were unchanged versus controls, indicating that indeed the NO_2-LDH/LDH ratio was increased.

Cardiac LDH nitration is lowered in eNOS-KO and MPO-KO mice.

We next wanted to address our second goal, to understand the mechanistic origin of the nitrogen in NO_2-LDH. Usually, it is assumed that protein nitration derives from peroxynitrite from the reaction between $^{\bullet}NO$ and $O_2^{\bullet-}$ [26]. However, another major source, not involving de novo NO synthesis is frequently overlooked, i.e. MPO-catalyzed nitration using nitrite in the presence of hydrogen peroxide [27] (Fig. 4a). To analyze this *in vivo*, we had to switch to mouse models, i.e. eNOS-KO and MPO-KO lines. Indeed, we observed that NO_2-LDH signals in heart tissue were not only reduced in eNOS-KO but also in MPO-KO mice when compared to their respective WT litter mates (Fig. 4b). These results therefore indicated that both pathways contribute to basal nitration of cardiac LDH. Moreover, we also compared LDH nitration to oxidation and showed that oxidation occurred at lower peroxynitrite concentrations and was half-maximal when LDH activity was still unchanged (Supplementary Fig. 2).

Further MALDI-TOF mass spectrometry analysis of the nitration site identifies the nitrated residue as tryptophan and not tyrosine.

A similarly frequent assumption about NO_2Tyr immunosignals is specificity with respect to the nitrated amino acid. Other nitration target amino acids, however, have been reported, most prominently tryptophan [28–30]. To identify the physiologically nitrated LDH residue(s), heart tissue was homogenized and subjected to 2D-PAGE in-gel digestion prior to MALDI-TOF MS analysis. Surprisingly, signals consistent with a nitrated tryptophan at position 324 of peptide 319-328 (SADTLWGIQK) of LDH (NO_2Trp-LDH) were detected (Fig. 5a). We cannot exclude nitration of other peptides of LDH that were below our level of detection. Nevertheless, our results strongly point to NO_2Trp being detected by the supposedly anti-NO_2Tyr pAb1.

NO_2Trp-LDH molecular dynamics simulations suggested higher restriction of the activity-essential interaction of the active site loop with the C-terminal α-helix.

Since we did observe a V_{max} effect on NO_2-LDH, we wanted to investigate whether there is a likely structural correlate for this via Trp-324. We therefore modeled the nitration into the structure of tetrameric and binary human LDH, and then performed molecular dynamics simulations. For distance metrics of human LDH and key structural components refer to Fig. 5b. The root-mean squared fluctuations (RMSF) of all atoms in each residue were averaged across the four subunits in each combined 3.5 μs trajectory (Supplementary Fig. 3). Subtracting the wildtype tetramer (WT) RMSF from the T4N (tetramer with NO_2Trp-324 residue on each subunit) highlighted differences in mobility between the dynamics of the WT compared with NO_2Trp-LDH (Fig. 5c). Positive values in the resulting graphs indicated greater mobility of residues in T4N compared with WT and *vice versa*. Moreover, distance histograms (Fig. 5d-e) show an increased mobility in the binary complexes compared with the ternary, expressed as a broadening of the histograms.

We found that NO_2Trp-LDH weakened the interaction between α-H and the active site loop. This decoupling led to a greater population of closed and “over-closed” states of the T4N active-site loop. By corollary, in WT LDH, the open active-site loop states are partly stabilized by interaction with the α-H helix. Therefore, nitration of LDH is expected to decrease LDH activity, consistent with our enzyme-kinetic findings (see Fig. 2d-e).

Discussion

We here close three major knowledge gaps in our understanding of protein nitration: specificity, origin, and disease relevance. With respect to the specificity of protein nitration, a vast heterogeneity of proteins are detected by supposedly uniform anti-NO_2Tyr antibodies. Moreover, tryptophan nitration (NO_2Trp) was a cofounding factor of our apparent NO_2Tyr-immunosignals. Protein NO_2Trp formation has been described in isolated proteins treated with H_2O_2/NO_2^- *in vitro* [31–34], peroxynitrite-exposed cells [35], and as physiological modification during aging in rat heart mitochondria [29]. Trp is an alternative target of nitration that deserves more attention [36,37] and immunosignals by anti-NO_2Tyr antibodies should rather be interpreted as NO_2Tyr/ NO_2Trp signals unless purified and chemically validated. Rebrin et al. [29] reported Trp nitration of succinyl-CoA:3-ketoacid CoA transferase (SCOT), which could not be reproduced by Wang et al. [38]. Whether Trp nitration has a functional consequence on SCOT remained unclear because both activation and inactivation were observed [29]. In hindsight, SCOT nitration is also the first documented example where Trp nitration has been mistaken as Tyr nitration based on cross-reactivity of a supposedly NO_2Tyr specific antibody [39], and many more of these examples may exist in the literature.

With respect to the origin of the nitrating nitrogen in NO_2Tyr/ NO_2Trp positive proteins, we show that both eNOS/NO and MPO/nitrite pathways, and possibly others, need to be equally considered and that the *a priori* assumption that NO_2Tyr immunosignals indicate NO scavenging by superoxide is not valid. Nevertheless, the effects of KO of eNOS and MPO are significant but not great. Previous data shows that NO modifications persist in the absence of active NO synthesis and dietary NOx intake (e.g., in eNOS$^{-/-}$ animals on a low-NOx diet and under the acute action of the NOS-inhibitor, L-NIO, or in Wistar rats on low-NOx diet with chronic administration of L-NMMA) [40]. Moreoever, NO levels remain essentially unchanged upon deletion of each NOS isoform. Accordingly, these findings

reflect the action of a compensatory mechanism that maintains basal levels of NO metabolites in tissues e.g. constant upregulation of remaining NOSs in an attempt to restore basal levels.

With respect to disease relevance, probably our most relevant finding is that protein tryptophan nitration is a physiological event. This represents a similar dogma shift as for ROS formation, which also should not be *a priori* considered as oxidative stress and a disease marker. Thus, both ROS and reactive nitrogen and protein nitration represent physiological events, even though they may be upregulated in disease as we show for diabetes and cardiac stress (see Fig. 3).

Not many specific functional consequences have been described for protein nitration. Assuming Trp nitration and activity modulation of both LDH (decreasing activity) and SCOT (increasing activity) would occur, this may be a protective mechanism, allowing the heart to better utilize ketone metabolism for energy production at a time when other metabolic processes may be diminished [28,29]. Molecular dynamics simulations were performed on NO_2-LDH, aiming to understand the impairment of the enzyme activity (see Fig. 5). While differences in activity between WT and T4N of a factor of two is significant in physiological terms, it corresponds to minor changes in the free energy states in the catalytic process. The catalytic cycle of LDH is a well understood ordered bi-bi reaction mechanism where substrate and product enter and leave the active-site, with concomitant closing and opening of the active-site loop, after cofactor binding. Detailed kinetic characterization of LDH from *Bacillus stearothermophilus* [41] and *Plasmodium falciparum* [42] has revealed this loop movement to be a rate limiting step in the reaction mechanism. Any perturbation of this delicately balanced conformational change is expected to compromise the catalytic activity of the enzyme. We suggest that conformational movement of the active-site loop in cardiac LDH is also a rate limiting step and the weakening of the interaction between this loop and the α-H helix in T4N (as described in our results) is

responsible for the impaired catalytic activity. Whether tryptophan nitration effects the conversion of either pyruvate or other 2-oxo/-2-hydroxy acids warrants further investigation.

Like many enzymes, LDH post-transcriptional activity is regulated by phosphorylation and acetylation of amino acid residues. The tyrosine kinase FGFR1 has been shown to directly phosphorylate LDH at Y10 and Y83 [43]. Y10 phosphorylation of LDH promotes active, tetrameric LDHA formation, whereas phosphorylation of Y83 promotes NADH substrate binding. Our finding obviously promotes the opposite, suggesting an antagonistic effects of tyrosine phosphorylation and tryptophan nitration. Inhibition of LDH reduces aerobic glycolysis, gene transcription, channel complex regulation, molecular chaperones and cell cycle regulation. Cells are then forced to use oxidative phosphorylation and pyruvate enters the mitochondria. This leads to reactive oxygen species (ROS) generation [44]. Since the nitration is already a ROS-induced event, this may be a mechanism of ROS-induced ROS formation [45], which in heart is protective triggering for example capillary density and angiogenesis [46,47].

In conclusion, cardiac LDH appears to be the first protein basally regulated by nitration and not only a loss-of-function biomarker of metabolic stress. NO_2-LDH has a lower V_{max} and the nitration is further increased under cardiac metabolic stress. Furthermore, *in vivo* NO_2Tyr immunoreactivity not necessarily reflects Tyr nitration or solely NO scavenging. Instead, it may indicate nitrite/MPO-dependent Trp nitration and physiological signaling. This has wide implications on re-interpreting previous data using NO_2Tyr immunoreactivity as a biomarker and on our understanding of nitration as a physiological protein modification and signaling mechanism.

Methods

Detailed experimental procedures are provided in Supplementary Methods.

Word count (main text without references): 2137 words.

References

1. Sies, H. Oxidative stress: a concept in redox biology and medicine. *Redox Biol.* **4,** 180–183 (2015).
2. Beckman, J. S. & Koppenol, W. H. Nitric oxide, superoxide, and peroxynitrite: the good, the bad, and ugly. *Am. J. Physiol. Physiol.* **271,** C1424-37 (1996).
3. Radi, R. Nitric oxide, oxidants, and protein tyrosine nitration. *Proc. Natl. Acad. Sci.* **101,** 4003–4008 (2004).
4. Armitage, M. E., Wingler, K., Schmidt, H. H. H. W. & La, M. Translating the oxidative stress hypothesis into the clinic: NOX versus NOS. *J. Mol. Med.* **87,** 1071–1076 (2009).
5. Viappiani, S. & Schulz, R. Detection of specific nitrotyrosine-modified proteins as a marker of oxidative stress in cardiovascular disease. *AJP Hear. Circ. Physiol.* **290,** H2167–H2168 (2006).
6. Shishehbor, M. H. & Hazen, S. L. Inflammatory and oxidative markers in atherosclerosis: Relationship to outcome. *Curr. Atheroscler. Rep.* **6,** 243–50 (2004).
7. Ho, E., Karimi Galougahi, K., Liu, C.-C., Bhindi, R. & Figtree, G. A. Biological markers of oxidative stress: Applications to cardiovascular research and practice. *Redox Biol.* **1,** 483–491 (2013).
8. Fernández, E., García-Moreno, J.-M., Martín de Pablos, A. & Chacón, J. May the Evaluation of Nitrosative Stress Through Selective Increase of 3-Nitrotyrosine Proteins Other Than Nitroalbumin and Dominant Tyrosine-125/136 Nitrosylation of Serum α-Synuclein Serve for Diagnosis of Sporadic Parkinson's Disease? *Antioxid. Redox Signal.* **19,** 912–918 (2013).
9. Halliwell, B. What nitrates tyrosine? Is nitrotyrosine specific as a biomarker of peroxynitrite formation in vivo? *FEBS Lett.* **411,** 157–160 (1997).
10. Ye, Y. Z., Strong, M., Huang, Z.-Q. Q. & Beckman, J. S. Antibodies that recognize

1 nitrotyrosine. *Methods Enzymol.* **269,** 201–209 (1996).
2 11. Reiter, C. D., Teng, R.-J. & Beckman, J. S. Superoxide Reacts with Nitric Oxide to
3 Nitrate Tyrosine at Physiological pH via Peroxynitrite. *J. Biol. Chem.* **275,** 32460–
4 32466 (2000).
5 12. Breusing, N. & Grune, T. Biomarkers of protein oxidation from a chemical, biological
6 and medical point of view. *Experimental Gerontology* (2010).
7 doi:10.1016/j.exger.2010.04.004
8 13. Sampson, J. B., Ye, Y., Rosen, H. & Beckman, J. S. Myeloperoxidase and
9 Horseradish Peroxidase Catalyze Tyrosine Nitration in Proteins from Nitrite and
10 Hydrogen Peroxide. *Arch. Biochem. Biophys.* **356,** 207–213 (1998).
11 14. Bigelow, D. J. Nitrotyrosine-modified SERCA2: a cellular sensor of reactive nitrogen
12 species. *Pflügers Arch. - Eur. J. Physiol.* **457,** 701–710 (2009).
13 15. Knyushko, T. V., Sharov, V. S., Williams, T. D., Schöneich, C. & Bigelow, D. J. 3-
14 Nitrotyrosine Modification of SERCA2a in the Aging Heart: A Distinct Signature of
15 the Cellular Redox Environment †. *Biochemistry* **44,** 13071–13081 (2005).
16 16. Li, H., Gutterman, D. D., Rusch, N. J., Bubolz, A. & Liu, Y. Nitration and Functional
17 Loss of Voltage-Gated K+ Channels in Rat Coronary Microvessels Exposed to High
18 Glucose. *Diabetes* **53,** 2436–2442 (2004).
19 17. Haddad, I. Y., Zhu, S., Ischiropoulos, H. & Matalon, S. Nitration of surfactant protein
20 A results in decreased ability to aggregate lipids. *Am. J. Physiol. Cell. Mol. Physiol.*
21 **270,** L281-8 (1996).
22 18. Ferrer-Sueta, G. *et al.* Biochemistry of Peroxynitrite and Protein Tyrosine Nitration.
23 *Chemical Reviews* (2018). doi:10.1021/acs.chemrev.7b00568
24 19. Akaike, T. *et al.* Pathogenesis of influenza virus-induced pneumonia: involvement of
25 both nitric oxide and oxygen radicals. *Proc. Natl. Acad. Sci.* **93,** 2448–2453 (1996).
26 20. Akaike, T. *et al.* 8-Nitroguanosine formation in viral pneumonia and its implication for

pathogenesis. *Proc. Natl. Acad. Sci.* **100,** 685–690 (2003).

21. Evans, T. J. *et al.* Cytokine-treated human neutrophils contain inducible nitric oxide synthase that produces nitration of ingested bacteria. *Proc. Natl. Acad. Sci.* **93,** 9553–9558 (1996).

22. Hayashi, T. *et al.* Modulating role of estradiol on arginase II expression in hyperlipidemic rabbits as an atheroprotective mechanism. *Proc. Natl. Acad. Sci.* **103,** 10485–10490 (2006).

23. Szabo, C. *et al.* Protection against peroxynitrite-induced fibroblast injury and arthritis development by inhibition of poly(ADP-ribose) synthase. *Proc. Natl. Acad. Sci.* **95,** 3867–3872 (1998).

24. Graham, M. L., Janecek, J. L., Kittredge, J. A., Hering, B. J. & Schuurman, H. J. The streptozotocin-induced diabetic nude mouse model: Differences between animals from different sources. *Comp. Med.* (2011). doi:10.1152/ajprenal.00292.2015

25. Berthiaume, J. M. & Wallace, K. B. Adriamycin-induced oxidative mitochondrial cardiotoxicity. in *Cell Biology and Toxicology* (2007). doi:10.1007/s10565-006-0140-y

26. Peluffo, G. & Radi, R. Biochemistry of protein tyrosine nitration in cardiovascular pathology. *Cardiovasc. Res.* **75,** 291–302 (2007).

27. van der Vliet, A., Eiserich, J. P., Halliwell, B. & Cross, C. E. Formation of Reactive Nitrogen Species during Peroxidase-catalyzed Oxidation of Nitrite. *J. Biol. Chem.* **272,** 7617–7625 (1997).

28. Nuriel, T., Hansler, A. & Gross, S. S. Protein nitrotryptophan: Formation, significance and identification. *J. Proteomics* **74,** 2300–2312 (2011).

29. Rebrin, I., Brégère, C., Kamzalov, S., Gallaher, T. K. & Sohal, R. S. Nitration of Tryptophan 372 in Succinyl-CoA:3-Ketoacid CoA Transferase during Aging in Rat Heart Mitochondria †. *Biochemistry* **46,** 10130–10144 (2007).

30. Souza, J. M., Peluffo, G. & Radi, R. Protein tyrosine nitration—Functional alteration or just a biomarker? *Free Radic. Biol. Med.* **45,** 357–366 (2008).

31. Suzuki, T. *et al.* Nitration and nitrosation of N-acetyl-l-tryptophan and tryptophan residues in proteins by various reactive nitrogen species. *Free Radic. Biol. Med.* **37,** 671–681 (2004).

32. Yamakura, F. & Ikeda, K. Modification of tryptophan and tryptophan residues in proteins by reactive nitrogen species. *Nitric Oxide* **14,** 152–161 (2006).

33. Yamakura, F. *et al.* Nitrated and Oxidized Products of a Single Tryptophan Residue in Human Cu,Zn-Superoxide Dismutase Treated with Either Peroxynitrite-Carbon Dioxide or Myeloperoxidase-Hydrogen Peroxide-Nitrite. *J. Biochem.* **138,** 57–69 (2005).

34. Yamakura, F., Matsumoto, T., Taka, H., Fujimura, T. & Murayama, K. 6-Nitrotryptophan: a specific reaction product of tryptophan residue in human Cu, Zn-SOD treated with peroxynitrite. *Adv. Exp. Med. Biol.* **527,** 745–9 (2003).

35. Ikeda, K. *et al.* Detection of 6-nitrotryptophan in proteins by Western blot analysis and its application for peroxynitrite-treated PC12 cells. *Nitric Oxide* **16,** 18–28 (2007).

36. Alvarez, B. *et al.* Peroxynitrite-Dependent Tryptophan Nitration. *Chem. Res. Toxicol.* **9,** 390–396 (1996).

37. Herold, S. Nitrotyrosine, dityrosine, and nitrotryptophan formation from metmyoglobin, hydrogen peroxide, and nitrite. *Free Radic. Biol. Med.* **36,** 565–579 (2004).

38. Wang, Y. *et al.* The Nitrated Proteome in Heart Mitochondria of the db/db Mouse Model: Characterization of Nitrated Tyrosine Residues in SCOT. *J. Proteome Res.* **9,** 4254–4263 (2010).

39. Marcondes, S., Turko, I. V & Murad, F. Nitration of succinyl-CoA:3-oxoacid CoA-

transferase in rats after endotoxin administration. *Proc. Natl. Acad. Sci.* **98,** 7146–7151 (2001).

40. Milsom, A. B., Fernandez, B. O., Garcia-Saura, M. F., Rodriguez, J. & Feelisch, M. Contributions of nitric oxide synthases, dietary nitrite/nitrate, and other sources to the formation of NO signaling products. *Antioxid. Redox Signal.* **17,** 422–32 (2012).

41. Wilks, H. M. *et al.* Designs for a broad substrate specificity keto acid dehydrogenase. *Biochemistry* **29,** 8587–8591 (1990).

42. Shoemark, D. K., Cliff, M. J., Sessions, R. B. & Clarke, A. R. Enzymatic properties of the lactate dehydrogenase enzyme from Plasmodium falciparum. *FEBS J.* **274,** 2738–2748 (2007).

43. Fan, J. *et al.* Tyrosine Phosphorylation of Lactate Dehydrogenase A Is Important for NADH/NAD+ Redox Homeostasis in Cancer Cells. *Mol. Cell. Biol.* (2011). doi:10.1128/MCB.06120-11

44. Liemburg-Apers, D. C., Willems, P. H. G. M., Koopman, W. J. H. & Grefte, S. Interactions between mitochondrial reactive oxygen species and cellular glucose metabolism. *Archives of Toxicology* (2015). doi:10.1007/s00204-015-1520-y

45. Zorov, D. B., Juhaszova, M. & Sollott, S. J. Mitochondrial Reactive Oxygen Species (ROS) and ROS-Induced ROS Release. *Physiol. Rev.* (2014). doi:10.1152/physrev.00026.2013

46. Nabeebaccus, A. A. *et al.* Nox4 reprograms cardiac substrate metabolism via protein O-GlcNAcylation to enhance stress adaptation. *JCI insight* (2017). doi:10.1172/jci.insight.96184

47. Zhang, M. *et al.* NADPH oxidase-4 mediates protection against chronic load-induced stress in mouse hearts by enhancing angiogenesis. *Proc. Natl. Acad. Sci.* (2010). doi:10.1073/pnas.1009700107

Acknowledgements

Work in A.J. laboratory was supported by BBSRC, BHF and MRC; in P.B. laboratory by NKFIH (K123975); in H.H.H.W.S. laboratory by an ERC Advanced Investigator Grant (294683 - RadMed), an ERC proof-of-concept grant (139-101052 - SAVEBRAIN) and the EU Horizon 2020 programme, REPO-TRIAL. The authors would like to thank G. Jansen for technical help, and Dr. P.M.H. Schiffers for carefully reading earlier stages of the manuscript. We also thank the Advanced Computing Research Centre at Bristol and BrisSynBio for access to the HPC machines BlueCrystal and BlueGem. We thank the HECBiosim Consortium for access to the UK National HPC facility Archer.

Author information

Affiliations

Department of Pharmacology and Personalised Medicine, Maastricht University, Maastricht, The Netherlands

Cristian Nogales, Ana I. Casas & Harald H.H.W. Schmidt.

Medtronic Bakken Research Center, Maastricht, The Netherlands

Jeroen Frijhoff

DiaSys Diagnostic Systems GmbH, Holzheim, Germany

Detlef Thoenges

School of Biochemistry, University of Bristol, Bristol, UK

Richard B. Sessions

Leibiniz-Institut für Analytische Wissenschaften – ISAS, Dortmund, Germany

Albert Sickmann

Rudolf-Buchheim-Institue for Pharmacology, Justus-Liebig-University, Giessen, Germany

Tatiana Nedvetskaya

School of Chemistry, Autonomous University of Querétaro. Querétaro, México

Cesar Ibarra-Alvarado

German Diabetes Research Institute, Düsseldorf, Germany

Vera Schmitz & Peter Rösen

Heinrich-Heine-University, Department Cardiovascular Physiology, Düsseldorf, Germany

Axel Goedecke

University of Nicosia Medical School, Nicosia, Cyprus

Aleksandar Jovanović

Merck Exploratory Science Center, Cambridge, Massachusetts

David H. Perlman

Cologne Cardiovascular Research Center CCRC, Cologne, Germany

Anna Klinke & Stephan Baldus

Department of Medical Chemistry, Faculty of Medicine, University of Debrecen, Debrecen, Hungary and MTA-DE Lendület Laboratory of Cellular Metabolism, Debrecen, Hungary

Péter Bai

Department of Oncology, Microbiology and Immunology; University of Fribourg, Fribourg, Switzerland

Csaba Szabo

University of Southampton Medical School, Southampton, UK

Martin Feelisch

Contributions

H.H.H.W.S. designed research; J.F., D.T., T.N., C.I.A., A.S., P.B., C.S., V.S., P.R., A.J., A.G., D.H.P., R.B.S. and M.F. performed research; A.S., A.G., A.K., S.B., D.H.P., M.F. and H.H.H.W.S. contributed new reagents/analytic tools; J.F., D.T., D.H.P., and H.H.H.W.S. analyzed data; and C.N., J.F., C.S., D.H.P., M.F., A.I.C. and H.H.H.W.S. wrote the paper.

Competing interests

The authors declare no conflict of interests.

Corresponding authors

Correspondence to Harald H.H.W. Schmidt or Cristian Nogales.

Data availability

Data available from the corresponding authors upon reasonable request.

1 **Figures and figure legends**

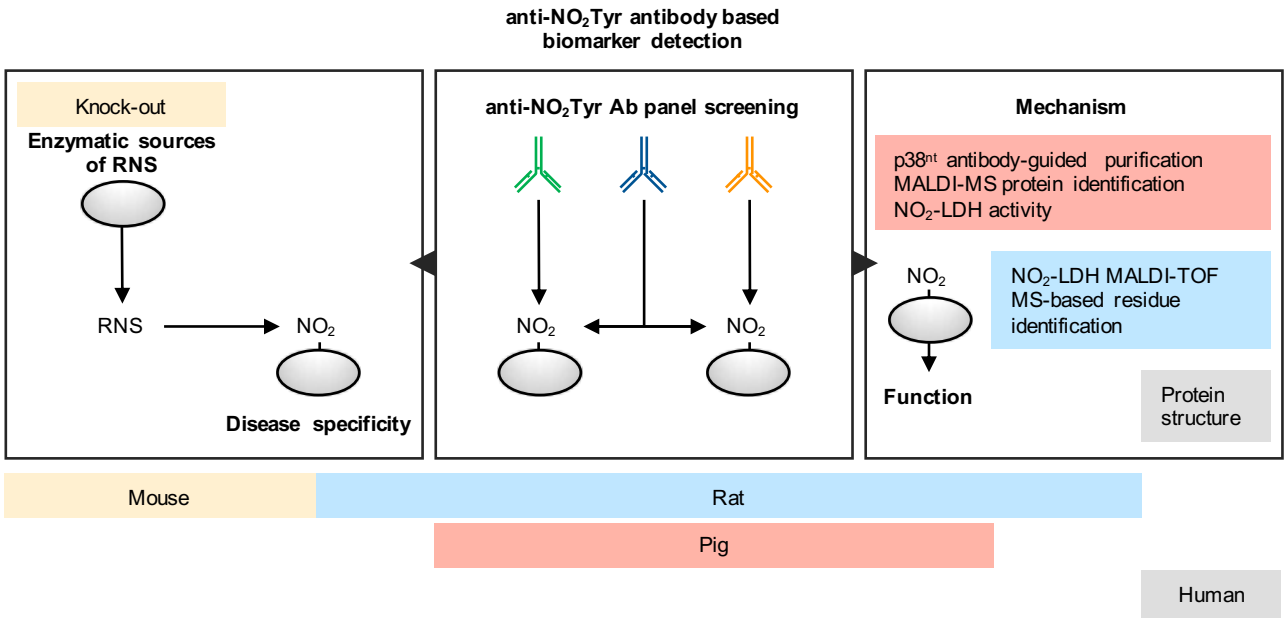

2

3 **Figure 1. Experimental outline for an anti-NO_2Tyr antibody-based biomarker**

4 **detection approach.** Central panel: Antibody panel screening, an anti-NO_2Tyr antibody

5 panel was tested in porcine and rat tissues under physiological conditions. Different

6 antibodies might recognize different nitrated proteins (green and orange antibodies) or one

7 antibody might detect more than one nitrated protein (blue antibody). Right panel: A 38

8 kDa band was especially prominent and, subsequently, purified in large mammals and

9 identified via MALDI-TOF as LDH. NO_2-LDH activity was also assessed. We identified the

10 nitrated residue and simulated the effect of the nitration in the protein structure and

11 mechanism using human LDH. Left panel: Different rodent models, as well as knock-out

12 mouse models were used to elucidate the effects of NO_2-LDH in disease, diabetes and

13 myocardial stress, and the enzymatic sources of reactive nitrogen species (RNS) leading

14 to LDH nitration, respectively.

15

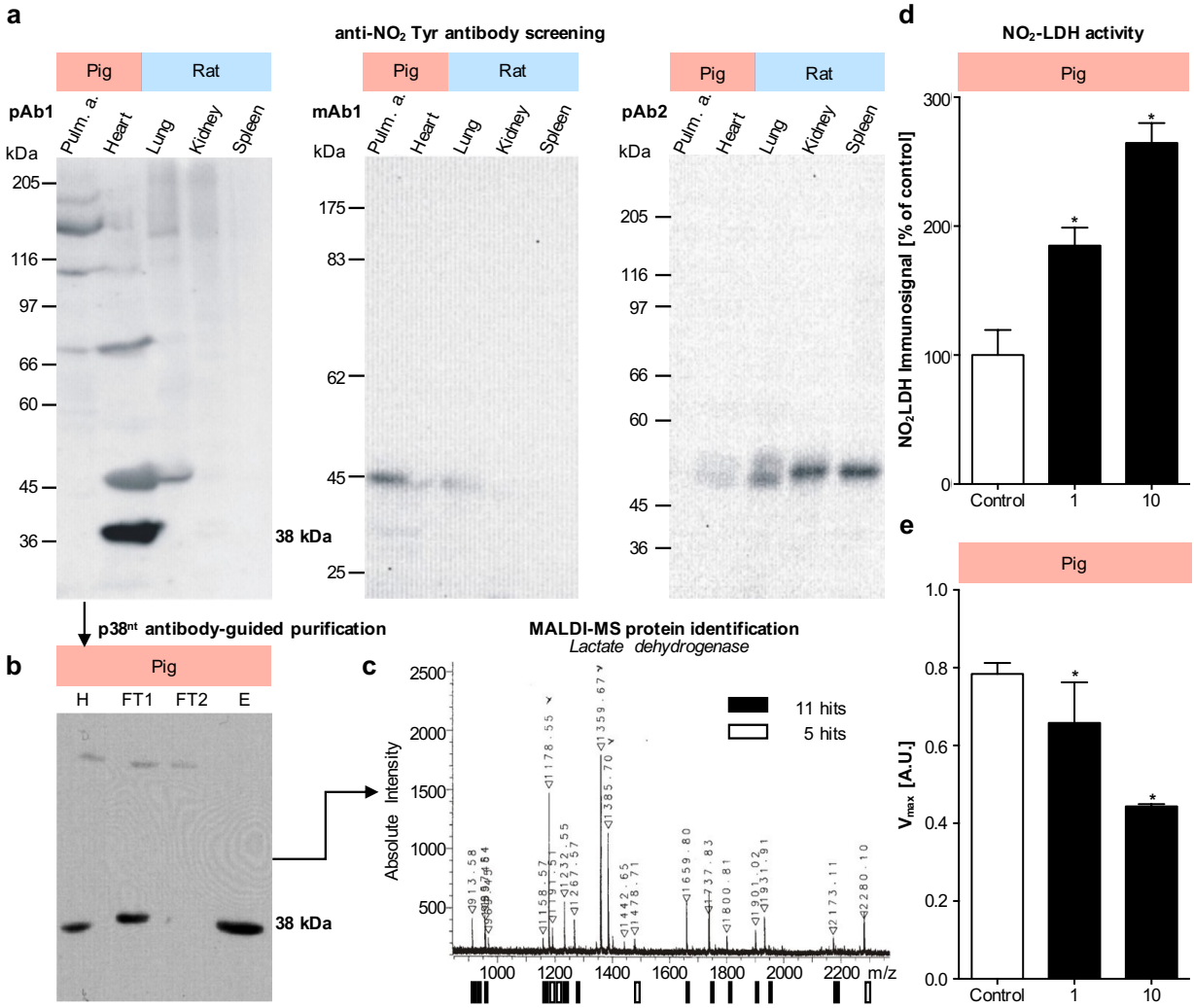

Figure 2. Screening of different native tissue homogenates identifies a 38 kDa band in heart as major physiologically NO_2Tyr-immuno positive protein. Further purification and MALDI-MS analysis identified the 38 kDa band as LDH. (**a**) Immunopositive pig and rat tissues from Fig S1 were further analyzed by SDS-PAGE under reducing conditions (dithiothreitol) and subsequent western blot. The band pattern was different for all three polyclonal (pAb) or monoclonal (mAb) antibodies: pAb1, mAb1 and pAb2. The most intense NO_2Tyr immunopositive protein band at approximately 38 kDa ($p38^{nt}$) was detected using pAb1 in heart. (**b**) $p38^{nt}$ was purified from porcine heart homogenate by affinity (Blue Sepharose) followed by ion-exchange (Q-Sepharose) chromatography. Purification steps were tracked via protein nitrotyrosine detection using pAb1. *(**c**)* Purified cardiac $p38^{nt}$ was cut out from the gel, digested with trypsin and

analyzed by mass spectrometry and peptide mass fingerprint analysis. Most peptide ions detected were matched to lactate dehydrogenase: 11 ions matched to LDH (■) out of a total of 20 detected, with 5 ions matching to the next best protein assignment, malate dehydrogenase (MDH, □), identifying $p38^{nt}$ as LDH with a $p<0.05$. (**d**) LDH nitration was assessed by quantitative western blot analysis using pAb1 (n=9). (**e**) Vmax[LDH] remained unchanged up to an equimolar peroxynitrite:LDH ratio, and then decreased at a ratio of 10 (n=8). Data represent means ±SEM.

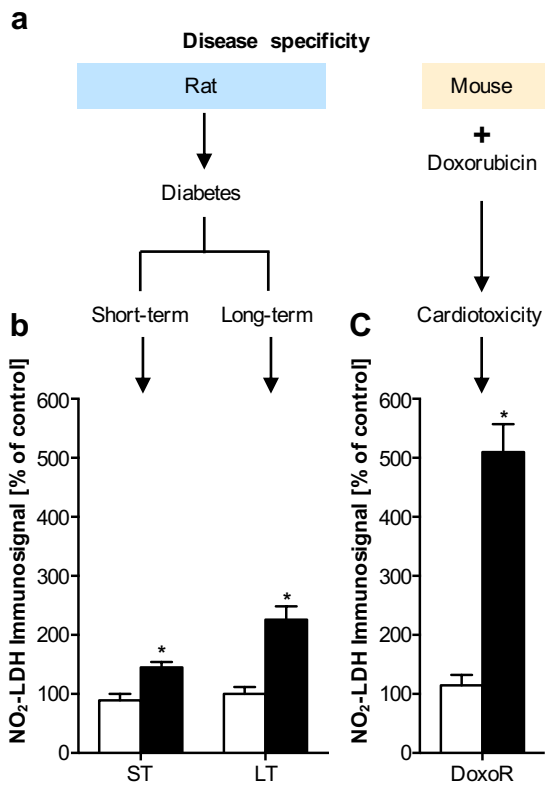

Figure 3. Pathological LDH nitration levels in short-term (ST) and long-term (LT) diabetic disease models and an oxidative stress myocardial dysfunction model. (**a**) Heart homogenates of ST and LT streptozotocin-treated diabetic rats or doxorubicin-treated mice (DoxoR) were analyzed by SDS-PAGE and immunoblot analysis for LDH nitration using the pAb1 antibody. In all three animal models, the relative NO_2-LDH signal intensity was increased. In diabetes, the long-term model yielded higher values than the short-term model, which may indicate either higher nitrosative stress, or, more likely, accumulation of LDH nitration (**b**). The highest increase was observed in the doxorubicin model (**c**). Data are expressed as % of untreated control animals (open bars) and represent means ± SEM of n=6-18 experiments.

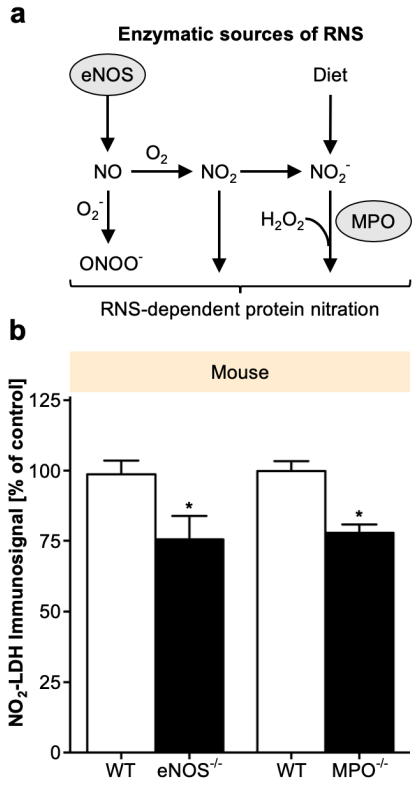

Figure 4. *In vivo* genetic validation of reactive nitrogen species (RNS) sources. (**a**) Events leading to oxidized and nitrated LDH. RNS (represented as $NO_2^-/H_2O_2/ONOO^-$) can nitrate LDH, resulting in decreased V_{max}. (**b**) Cardiac tissue was obtained from endothelial nitric oxide synthase (eNOS) and myeloperoxidase (MPO) knock-out (KO), and the respective wild-type (WT), mice. Basal nitration of LDH ($p38^{nt}$) was analyzed by immunoblot, and immunosignals quantified densitometrically. Data are expressed as % of control (i.e., of the respective WT animals) and represent means ± SEM of n=3-5 animals. NO_2-LDH depended on both eNOS and MPO.

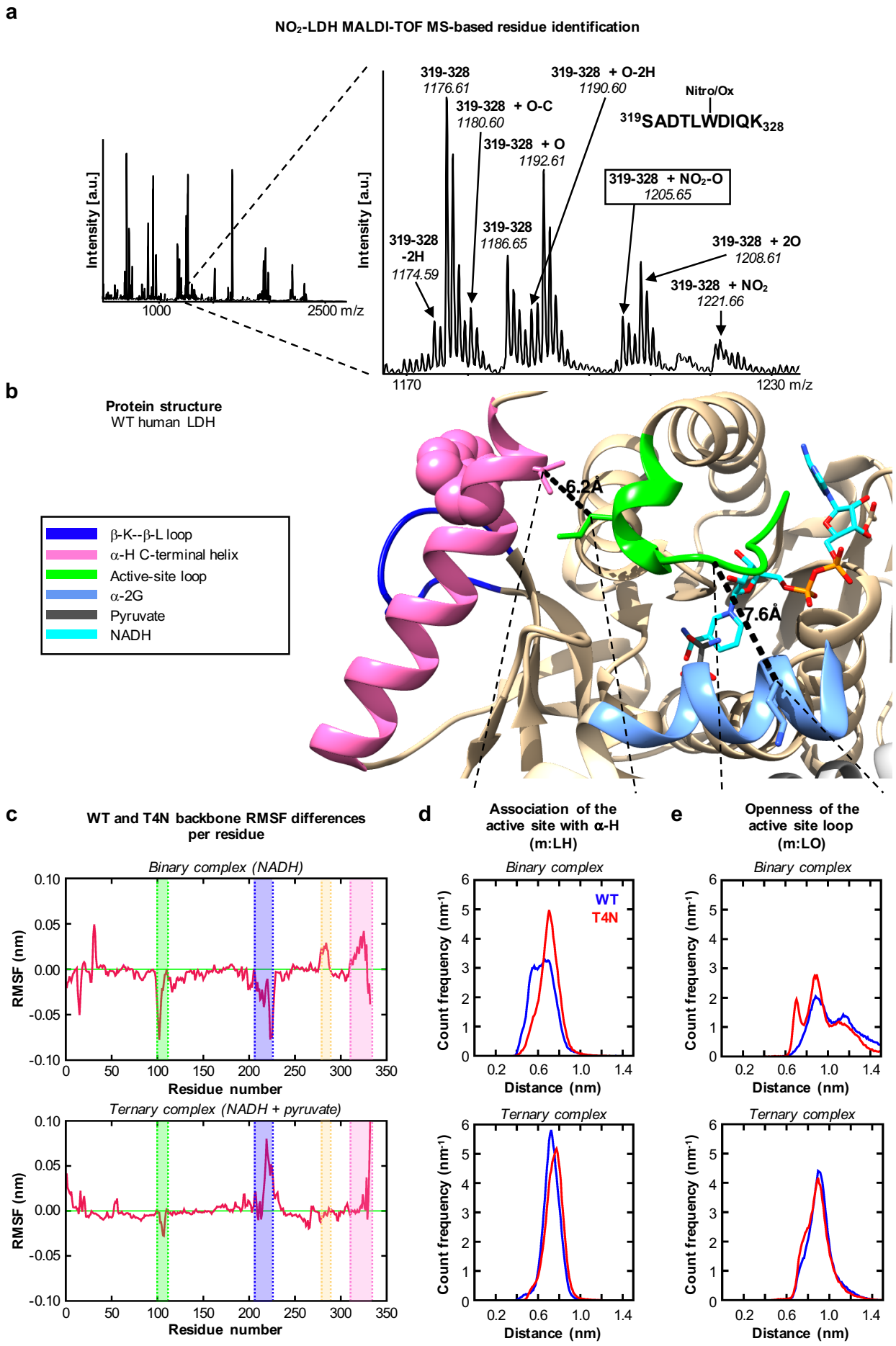
a
NO2-LDH MALDI-TOF MS-based residue identification
Intensity [a.u.]
1000
2500 m/z
319-328
1176.61
319-328 + O-2H
1190.60
Nitro/Ox
319-328 + O-C
1180.60
319-328 + O
1192.61
319-328 + NO2-O
1205.65
319-328
1186.65
319-328
-2H
1174.59
319-328 + 2O
1208.61
319-328 + NO2
1221.66
1170
1230 m/z
b
Protein structure
WT human LDH
β-K--β-L loop
α-H C-terminal helix
Active-site loop
α-2G
Pyruvate
NADH
6.2Å
7.6Å
c
WT and T4N backbone RMSF differences per residue
Binary complex (NADH)
Ternary complex (NADH + pyruvate)
RMSF (nm)
Residue number
d
Association of the active site with α-H (m:LH)
Binary complex
Ternary complex
WT
T4N
Count frequency (nm-1)
Distance (nm)
e
Openness of the active site loop (m:LO)
Binary complex
Ternary complex
Count frequency (nm-1)
Distance (nm)

1

Figure 5. Identification of LDH Trp-324 as physiologically nitrated and oxidized. The interaction of the active site loop with the C-terminal α-helix is essential and restricted in NO_2Trp-LDH. (**a**) Rat heart homogenate was subjected to 2D-PAGE and Coomasie staining; spots were subjected to in-gel digestion and MALDI-TOF MS analysis. Leftft panel: Mass spectrum derived from a spot corresponding to rat LDH over the range m/z 600 to 2700. Right panel: An expansion of the same spectrum over the range m/z 1170 to 1230, showing peptide ions assigned primarily to the peptide 319-328 (319SADTLWDIQK328), and its oxidized and nitrated derivatives. Major peptide ions are labeled with their observed m/z values and corresponding LDH mature protein amino acid intervals, as assigned by Mascot™, and additionally by manual comparison to predicted values calculated from the LDH sequence and oxidative and nitrative modifications. The ions correspond to the peptide 319-328 Trp (W)-nitrated species (319-328 + NO2) and its typical high energy decomposition product (319-328 + NO_2-O), as well as ions corresponding to the characteristic family of Trp oxidation forms, hydroxytryptophan (319-328 + Ox), didehydro-hydroxytryptophan (319-328 + Ox-2H), dihydroxytryptophan (319-328 + 2Ox), and kynurenin (319-328 + Ox-C). Other peptide ions display single (+ Ox) and double (+ 2Ox) oxidation, or didehydrogenation (- 2H). (**b**) Distance metrics mapped onto the crystal structure of WT (1I0Z). Color scheme: β-K--β-K loop, dark blue; α-helix, pink; active-site loop, green; α-2G, light blue; pyruvate, grey; NADH, cyan. Residue Trp-324 is shown in space filling. (**c**) Plot of the differences between T4N and WT backbone RMSF per residue (T4N – WT) in the binary complex. Structures are highlighted using the same color scheme as previously described plus the juxtaposed loop to the C-terminal α-helix which is highlighted in light orange. (**d** – **e**) Histograms of the distribution of distances. Blue WT; Red T4N. Metrics m:LH (107:CB-326:CB) showing the juxtaposition of the active-site loop and α-C-terminal helix and m:LO (103:CA-243:CB) showing the open/closed state of the active-site loop.

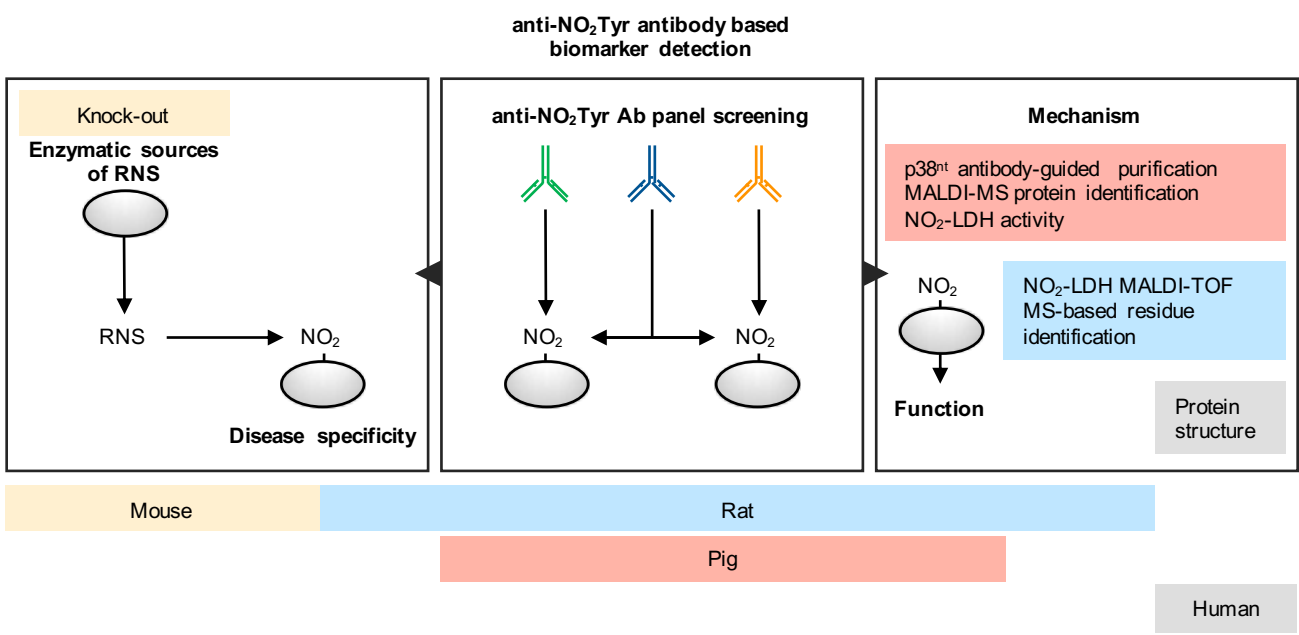
anti-NO2Tyr antibody based biomarker detection
Knock-out
Enzymatic sources of RNS
RNS
NO2
Disease specificity
anti-NO2Tyr Ab panel screening
NO2
NO2
Mechanism
p38nt antibody-guided purification
MALDI-MS protein identification
NO2-LDH activity
NO2
NO2-LDH MALDI-TOF MS-based residue identification
Function
Protein structure
Mouse
Rat
Pig
Human

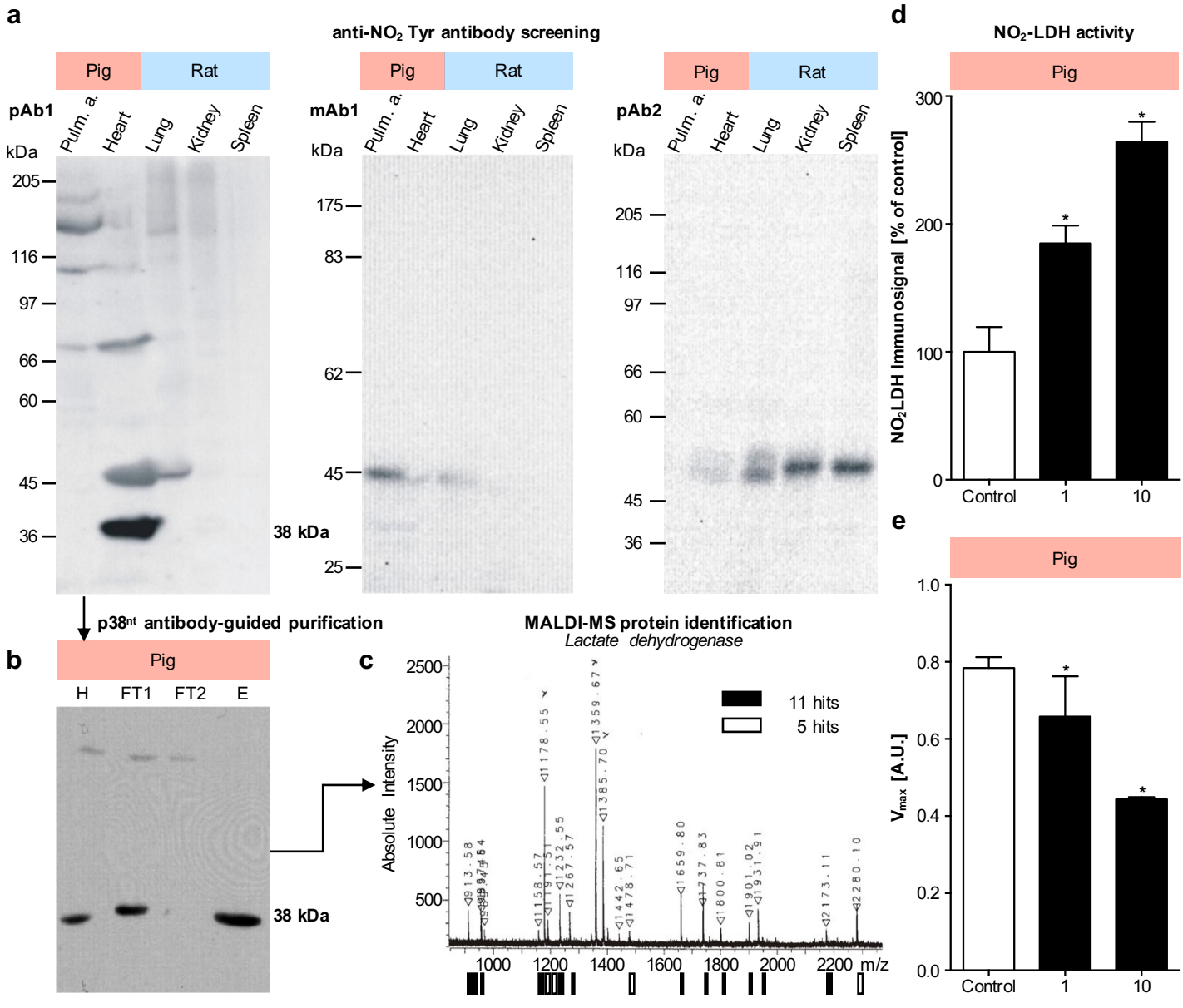
a
anti-NO2 Tyr antibody screening
Pig
Rat
pAb1
mAb1
pAb2
Pulm. a.
Heart
Lung
Kidney
Spleen
kDa
205
116
97
66
60
45
36
175
83
62
25
38 kDa
p38nt antibody-guided purification
b
H
FT1
FT2
E
c
MALDI-MS protein identification
Lactate dehydrogenase
Absolute Intensity
11 hits
5 hits
m/z
d
NO2-LDH activity
NO2LDH Immunosignal [% of control]
Control
1
10
e
Vmax [A.U.]

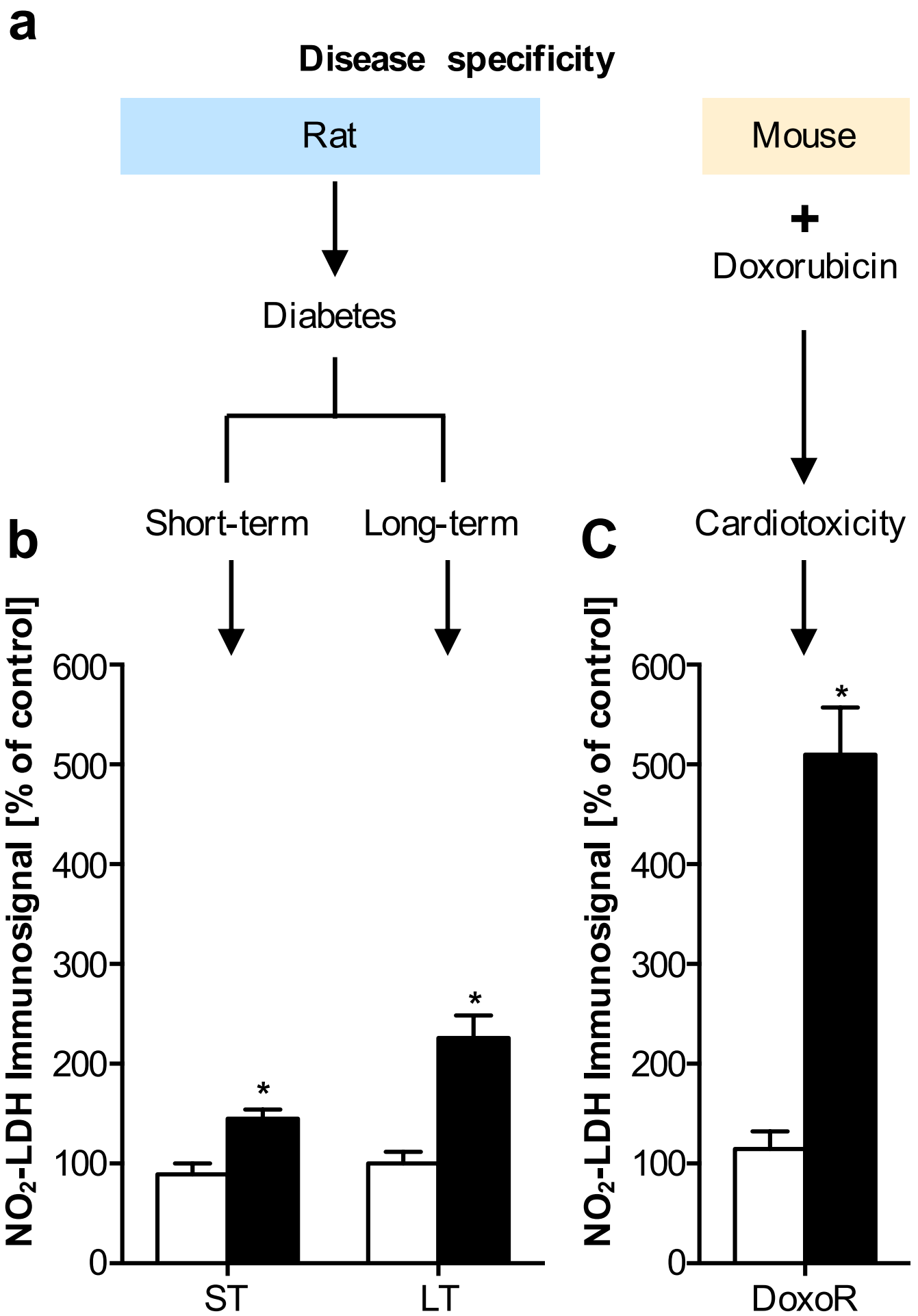
a
Disease specificity
Rat
Mouse
+
Doxorubicin
Diabetes
Short-term
Long-term
Cardiotoxicity
b
C
NO2-LDH Immunosignal [% of control]
600
500
400
300
200
100
0
*
ST
LT
DoxoR

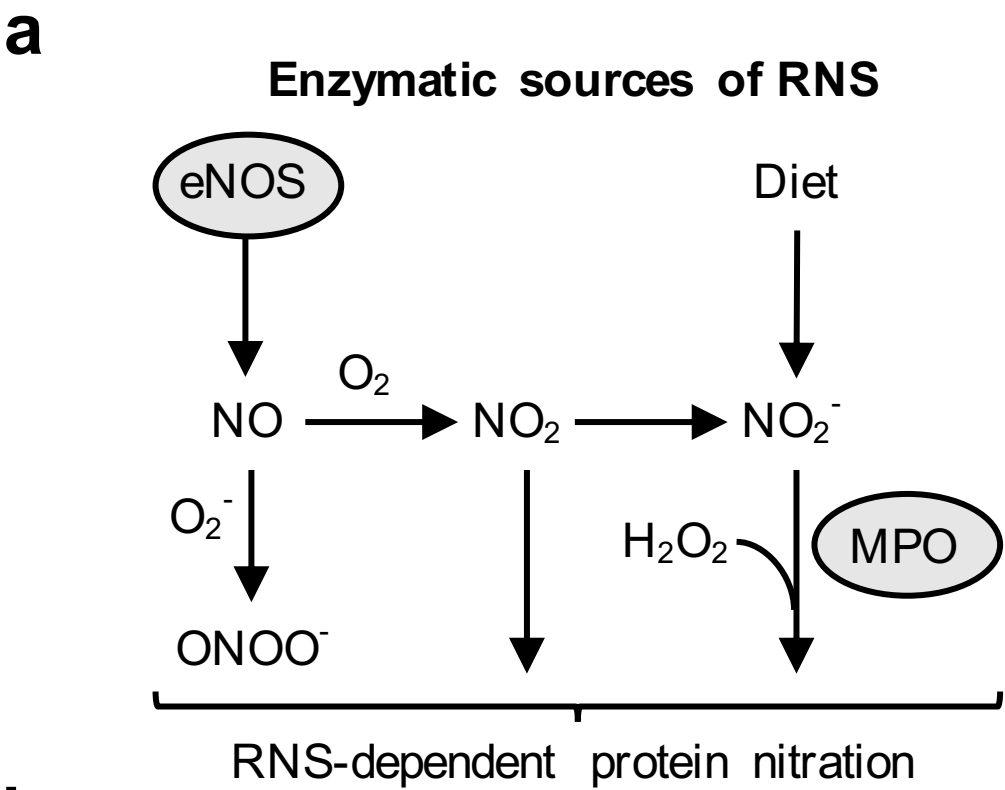
a
Enzymatic sources of RNS
eNOS
Diet
NO
O2
NO2
NO2-
O2-
H2O2
MPO
ONOO-
RNS-dependent protein nitration

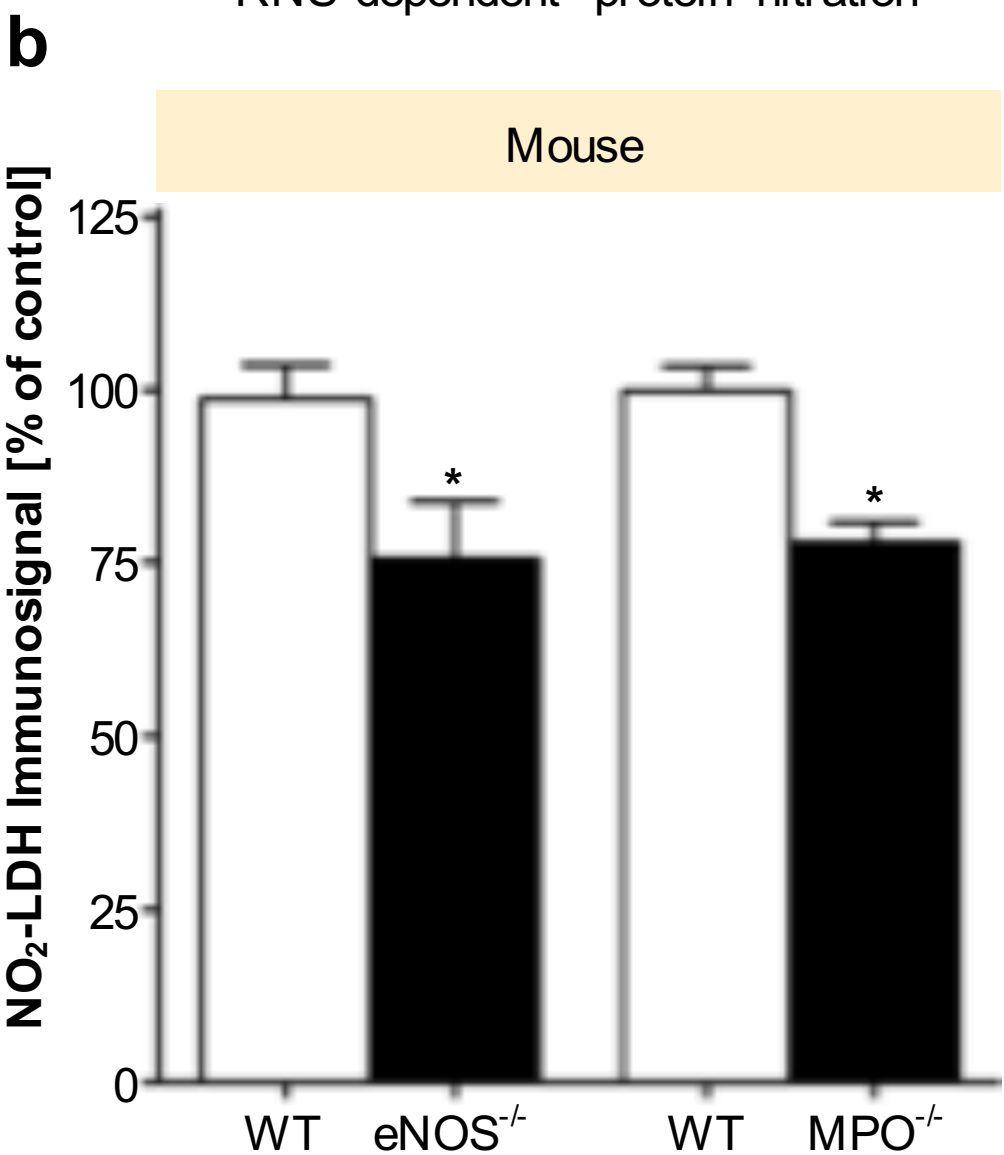
b
Mouse
NO2-LDH Immunosignal [% of control]
125
100
75
50
25
0
*
*
WT
eNOS-/-
WT
MPO-/-

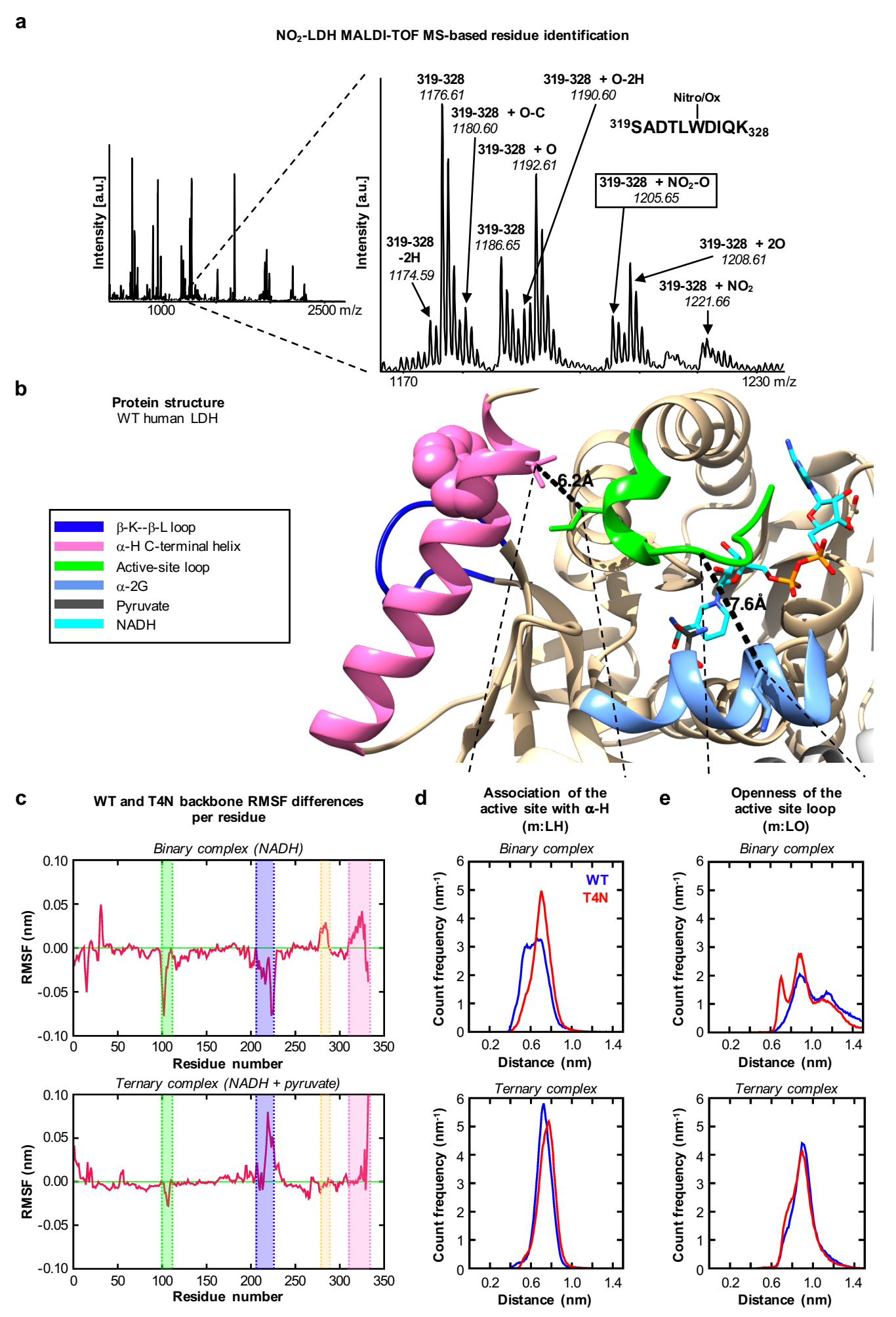
a
NO2-LDH MALDI-TOF MS-based residue identification
Intensity [a.u.]
1000
2500 m/z
319-328
1176.61
319-328 + O-2H
1190.60
Nitro/Ox
319-328 + O-C
1180.60
319SADTLWDIQK328
319-328 + O
1192.61
319-328 + NO2-O
1205.65
319-328
1186.65
319-328
-2H
1174.59
319-328 + 2O
1208.61
319-328 + NO2
1221.66
1170
1230 m/z
b
Protein structure
WT human LDH
β-K--β-L loop
α-H C-terminal helix
Active-site loop
α-2G
Pyruvate
NADH
6.2Å
7.6Å
c
WT and T4N backbone RMSF differences per residue
Binary complex (NADH)
Ternary complex (NADH + pyruvate)
RMSF (nm)
Residue number
d
Association of the active site with α-H (m:LH)
Binary complex
Ternary complex
WT
T4N
Count frequency (nm-1)
Distance (nm)
e
Openness of the active site loop (m:LO)
Binary complex
Ternary complex
Count frequency (nm-1)
Distance (nm)

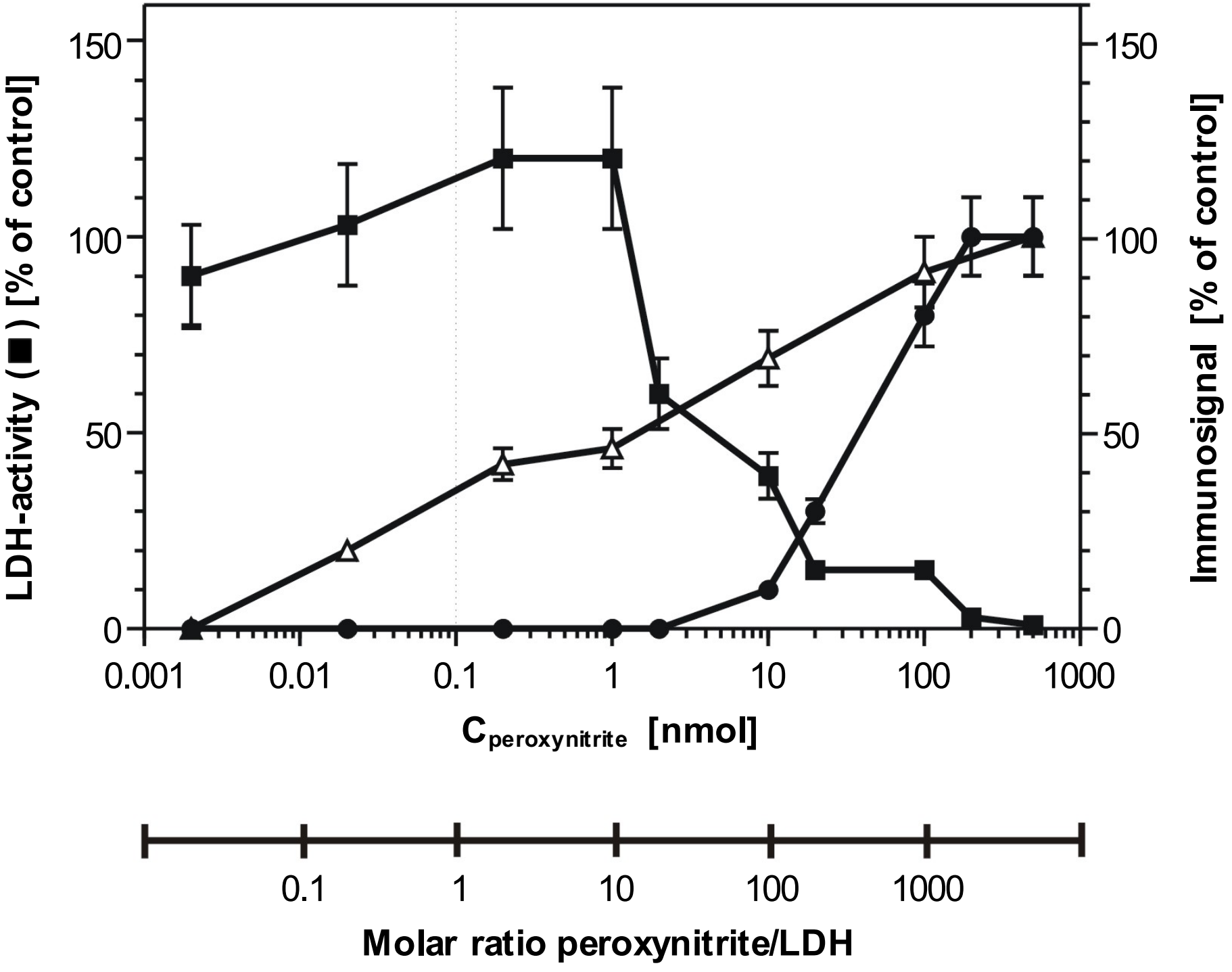
LDH-activity (■) [% of control]
Immunosignal [% of control]
150
100
50
0
0.001
0.01
0.1
1
10
100
1000
C peroxynitrite [nmol]
0.1
1
10
100
1000
Molar ratio peroxynitrite/LDH

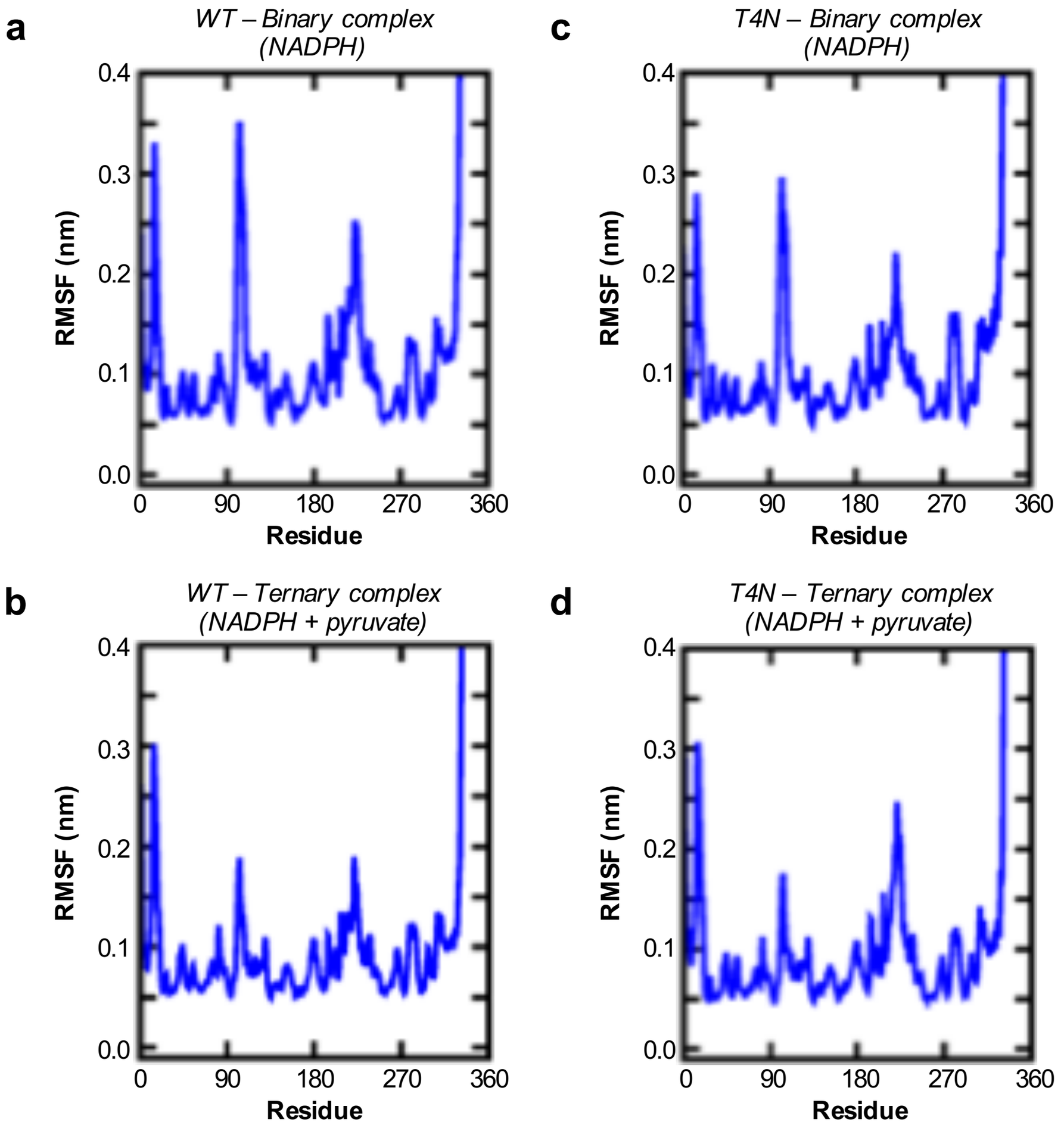
a
WT – Binary complex
(NADPH)
c
T4N – Binary complex
(NADPH)
b
WT – Ternary complex
(NADPH + pyruvate)
d
T4N – Ternary complex
(NADPH + pyruvate)
RMSF (nm)
0.0
0.1
0.2
0.3
0.4
Residue
0
90
180
270
360